



Electric field-induced tuning of magnetism in $\text{PbFe}_{0.5}\text{Nb}_{0.5}\text{O}_3$ at room temperature

S. Rayaprol, S. Mukherjee, S. D. Kaushik, S. Matteppanavar, and B. Angadi

Citation: *Journal of Applied Physics* **118**, 054103 (2015); doi: 10.1063/1.4928149

View online: <http://dx.doi.org/10.1063/1.4928149>

View Table of Contents: <http://scitation.aip.org/content/aip/journal/jap/118/5?ver=pdfcov>

Published by the [AIP Publishing](http://www.aip.org)

Articles you may be interested in

Scandium induced structural transformation and B'B" cationic ordering in $\text{Pb}(\text{Fe}_{0.5}\text{Nb}_{0.5})\text{O}_3$ multiferroic ceramics

J. Appl. Phys. **116**, 034104 (2014); 10.1063/1.4890020

Room temperature multiferroic properties of $\text{Pb}(\text{Fe}_{0.5}\text{Nb}_{0.5})\text{O}_3\text{-Co}_{0.65}\text{Zn}_{0.35}\text{Fe}_2\text{O}_4$ composites

J. Appl. Phys. **114**, 234106 (2013); 10.1063/1.4847595

Investigations on electrical and magnetic properties of multiferroic $[(1-x)\text{Pb}(\text{Fe}_{0.5}\text{Nb}_{0.5})\text{O}_3-x\text{Ni}_{0.65}\text{Zn}_{0.35}\text{Fe}_2\text{O}_4]$ composites

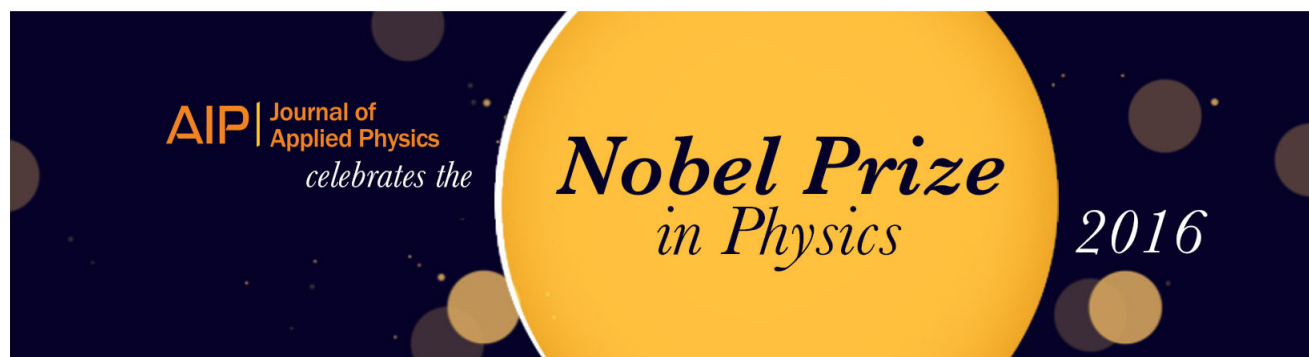
J. Appl. Phys. **113**, 144104 (2013); 10.1063/1.4799414

Field-induced changes in polarization and magnetization in $\text{Tb}_{0.3}\text{Dy}_{0.7}\text{Fe}_2/\text{PZT}$ laminate composite

J. Appl. Phys. **111**, 043906 (2012); 10.1063/1.3684984

Magnetoelectric coupling study in multiferroic $\text{Pb}(\text{Fe}_{0.5}\text{Nb}_{0.5})\text{O}_3$ ceramics through small and large electric signal standard measurements

J. Appl. Phys. **109**, 094106 (2011); 10.1063/1.3585757



Electric field-induced tuning of magnetism in $\text{PbFe}_{0.5}\text{Nb}_{0.5}\text{O}_3$ at room temperature

S. Rayaprol,^{1,a)} S. Mukherjee,¹ S. D. Kaushik,¹ S. Matteppanavar,² and B. Angadi^{2,a)}

¹UGC-DAE Consortium for Scientific Research—Mumbai Centre, R5 Shed, Trombay, Mumbai 400085, India

²Department of Physics, Bangalore University, Jnanabharathi Campus, Bengaluru 560056, India

(Received 26 June 2015; accepted 25 July 2015; published online 6 August 2015)

We study the influence of electrical poling, carried out at room temperature, on the structure and magnetism of $\text{Pb}(\text{Fe}_{0.5}\text{Nb}_{0.5})\text{O}_3$ by analyzing the differences observed in structural and magnetic properties before and after the electrical poling. The changes observed in magnetization of $\text{Pb}(\text{Fe}_{0.5}\text{Nb}_{0.5})\text{O}_3$ before and after electrical poling exhibit considerably strong converse magnetoelectric effect at room temperature. In addition, the strengthening of Fe/Nb-O bond due to electrical poling is discussed on the basis of Raman spectral studies and analysis of neutron diffraction patterns. The potential tunability of magnetization with electrical poling can be an ideal tool for realization of application potential of this multiferroic material. © 2015 AIP Publishing LLC. [<http://dx.doi.org/10.1063/1.4928149>]

I. INTRODUCTION

Recently, significant experimental efforts are focused on multiferroic (MF) heterostructures based on the tunability of their polarized or magnetic state through magnetoelectric or converse magnetoelectric couplings.^{1–6} Controlling magnetization or the magnetic anisotropy directly by using an electric field in MF is garnering attention over the traditional magnetic field control of electric polarization induced by spin polarized current.^{1–6} More precisely, an electric field induces elastic strain via ferroelectric domain reconfiguration.⁷ The induced strain is then transferred into magnetic domain, thus enabling good control of the magnetic properties.

In the present work, an electric field tunable (*ex-situ*) room temperature magnetic properties including magnetic hysteresis loop were studied in multiferroic $\text{Pb}(\text{Fe}_{0.5}\text{Nb}_{0.5})\text{O}_3$ (PFN). Owing to its unique complexities in structural (monoclinic, S.G: *Cm*) and physical properties, viz., ferroelectric ordering around Curie temperature (T_C) \sim 380 K and antiferromagnetic ordering around \sim 150 K, PFN has been subject of investigations for a long time by various research groups.^{8–13} Additionally, the influence of electrical poling on magnetization is also discussed by analyzing the neutron diffraction (ND) measurement and Raman spectroscopy studies. Such result provides the fundamental knowledge for development and designing of new generation devices.

II. EXPERIMENTAL DETAILS

The samples studied in this work have been prepared using a single step method as described earlier in detail of our recent publication.¹³ Room temperature neutron diffraction pattern was recorded before and after poling the sample in pellet form, on focusing crystal based powder

diffractometer (PD-3) at Dhruva reactor, Trombay using a neutron beam of wavelength 1.48 Å.¹⁴ Temperature dependent magnetization study and magnetic hysteresis at room temperature were also carried out on poled and unpoled samples using a 9 T PPMS-vibrating sample magnetometer (Quantum Design, USA). Raman spectra were also collected on poled and unpoled samples at room temperature using Ocean Optics ID Raman micro Raman spectrometer (Dunedin, USA) with a backscattering configuration, and the excitation laser with a wavelength of 785 nm and an output power of 70 mW. Electrical poling was done at room temperature using a customized sample cell connected to a high voltage *dc* power supply unit. The cell with electrodes was immersed in oil bath (Pure Silicone fluid) while poling the sample. The electric field applied for poling the samples for the present study was 5 kV/cm. Previous P-E measurements on PFN sample show that the coercive field at 50 Hz for this compound is \sim 10 kV/cm.¹³ In order to obtain large piezoelectric effect, it has been reported that poling the sample below its coercive field is advantageous.¹⁵ Therefore, for the present study, we poled the sample with an electric field of 5 kV/cm.

III. RESULTS AND DISCUSSION

In Fig. 1, we show the magnetization loop (M vs. H) measured on unpoled and poled samples at room temperature. The figure clearly shows the drastic change in magnetization behavior. In the unpoled sample, there is a weak ferromagnetic component present, which results in a hysteresis loop with a coercive field of around 400 Oe. Though the sample does not saturate till the highest measured field,¹³ the loop closes around 3 kOe. There is no linear variation of M with respect to H up to 5 kOe, and the magnitude of the magnetic moment at 5 kOe for the unpoled sample is about $0.003 \mu_B/\text{f.u.}$ In the case of poled sample, the changes are clearly visible, as the hysteresis loop has dramatically collapsed but there is reduction in the magnetic moment value to $0.002 \mu_B/\text{f.u.}$ at 5 kOe. Importantly,

^{a)} Authors to whom correspondence should be addressed. Electronic addresses: sudhindra@csr.res.in, Tel.: +91-22-25594727, Fax: +91-22-25505402 and brangadi@gmail.com, Tel.: +91-80-2296 1478, Fax: +91-80-2321 9295

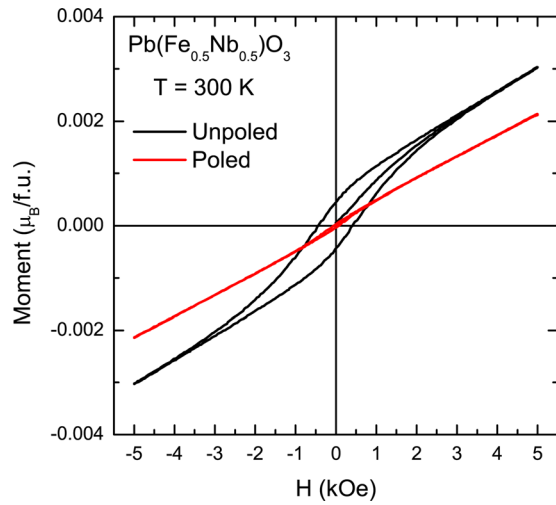


FIG. 1. Room temperature magnetization loops for unpoled and poled samples of $\text{Pb}(\text{Fe}_{0.5}\text{Nb}_{0.5})\text{O}_3$ sample.

PFN exhibits a considerably strong converse magnetoelectric effect (CME), $\sim 55\%$, defined here as $\text{CME}(\%) = \{[M(E) - M(0)]/M(0)\}(\%)$, where $M(E)$ and $M(0)$ represent magnetization with poled and unpoled sample, respectively (shown in Fig. 2).

The magnetic susceptibility measurements carried out in a field of 500 Oe and as a function of temperature between 5 K and 350 K are shown in Fig. 3. The PFN compound undergoes antiferromagnetic ordering around 150 K and another transition around 10 K.^{13,16} Though there is no change in the magnetic ordering temperatures (marked by the vertical lines) when unpoled samples data are compared with poled ones, the difference is apparent in the magnitude of the susceptibility value. There is decrease in the value for the poled sample.

The influence of the poling on the magnetism is clearly seen in Fig. 4. Here, the anisotropy that is the difference in

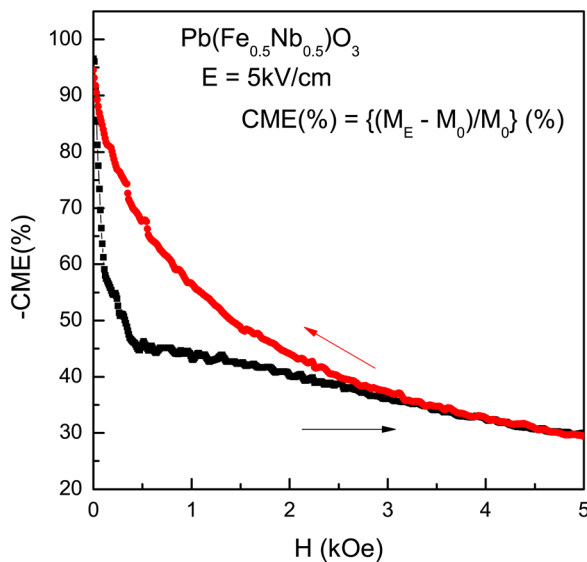


FIG. 2. CME, defined here as $\text{CME}(\%) = \{[M(E) - M(0)]/M(0)\}(\%)$, where $M(E)$ and $M(0)$ are magnetization values for poled and unpoled sample is plotted here as a function of the applied magnetic field. Only one quadrant data are shown here.

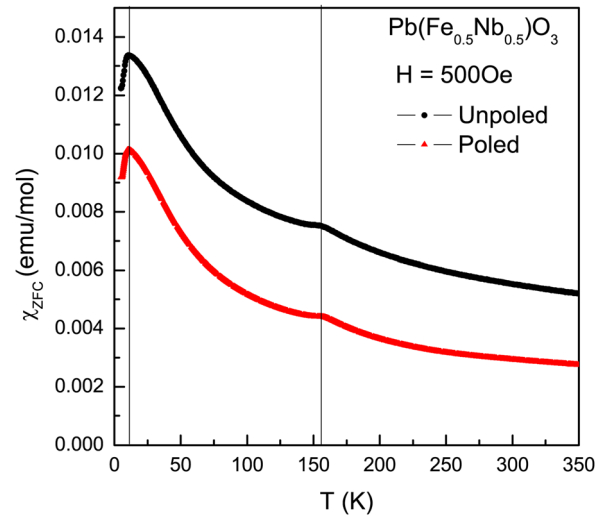


FIG. 3. dc magnetic susceptibility ($\chi = M/H$) for unpoled and poled samples of $\text{Pb}(\text{Fe}_{0.5}\text{Nb}_{0.5})\text{O}_3$ sample after zero field cooling to the lowest temperature. $\chi(T)$ has been measured while warming in a field of 500 Oe.

magnetic susceptibility measured in field cooled and zero field cooled state of the sample is plotted for both unpoled and poled sample. As the temperature is decreased from 350 K, there is negligible difference in both the samples. However as the temperature decreases below T_N (~ 150 K), the difference is clearly seen. This indicates that when the sample is poled, the magnetic anisotropy is reduced. It can thus be said that, with poling, the ferroelectric order becomes stronger and the magnetic order is slightly compromised. This clearly shows that the magnetic properties can be controlled by using the electric field.

In order to observe the influence of electrical polling on structural parameters, such as cell constants and bond-lengths, we carried out ND measurements on the unpoled and the poled samples which are shown in Fig. 5. For refining the pattern, the structure reported (for unpoled sample) in

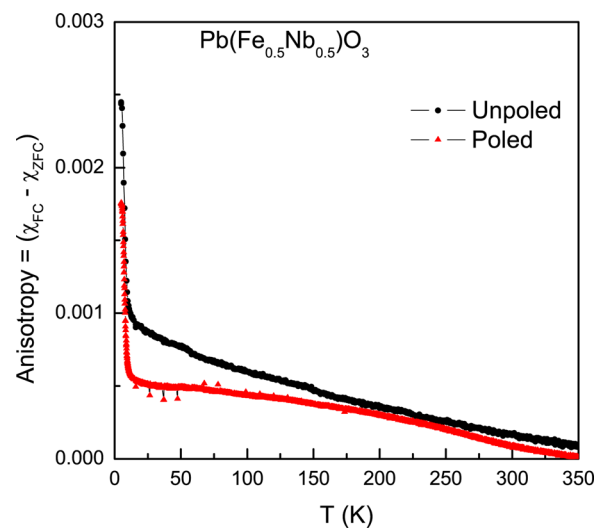


FIG. 4. The magnetic anisotropy given here as the difference between the magnetic susceptibility measured in field cooled state and zero field cooled state of the sample ($\text{Anisotropy} = \chi_{FC} - \chi_{ZFC}$) is plotted here for unpoled and poled samples of $\text{Pb}(\text{Fe}_{0.5}\text{Nb}_{0.5})\text{O}_3$.

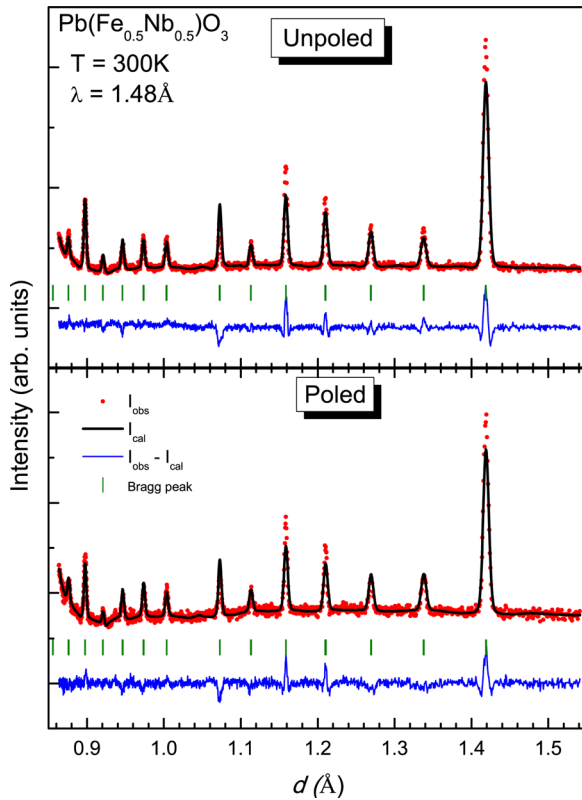


FIG. 5. Room temperature neutron diffraction patterns for $\text{Pb}(\text{Fe}_{0.5}\text{Nb}_{0.5})\text{O}_3$ sample before (unpoled) and after (poled) dc poling. The Rietveld analysis was carried out on both the patterns to ascertain the changes in cell parameters and atomic positions as a result of poling.

Ref. 13 has been taken as the starting model. The structure for the unpoled sample is monoclinic, space group Cm . Though no appreciable changes are visible in the ND pattern between poled and unpoled sample, the values of refined cell parameters, bond-lengths, and bond-valence sums, mentioned in Tables I and II, give indications of changes at the microscopic level when the sample is poled. There is marginal change in the cell volume and other cell parameters, with the volume increasing fractionally after poling. In Table III, the changes in the bond-lengths of Fe/Nb-O before and after poling are shown. It is clearly evident that there is significant influence of poling on the Fe/Nb-O polyhedra, resulting in large distortion around it. As seen in Fig. 1, the changes in magnetization value can thus be attributed to the changes in Fe/Nb-O polyhedra due to the poling, where the electrical poling changes the Fe-O bond length, influencing the magnetic properties.

Raman scattering spectroscopy is an effective tool to study the local structure of materials. In Fig. 6, the room temperature Raman spectra of poled and unpoled PFN are shown. There are ten lines observed for unpoled PFN at 242.7, 281.1,

TABLE II. Polyhedra distortion and Bond valence sums for various cations and anions of PFN before and after poling. These values have been obtained from Rietveld analysis of the ND patterns.

Atom	Valence	Distortion ($\times 10^{-4}$)		Bond valence sum	
		Unpoled	Poled	Unpoled	Poled
Pb	2.00	10.246	8.565	1.447(2)	1.384(1)
Fe	3.00	0.421	24.209	3.047(3)	3.172(3)
Nb	5.00	0.421	24.209	4.594(5)	4.783(4)
O1	-2.00	280.435	288.234	1.831(2)	1.820(1)
O2	-2.00	216.533	261.652	1.718(2)	1.771(2)

TABLE III. Changes in the Fe/Nb-O bond as a result of poling are tabulated here.

Atom	Bond length (\AA)	
	Unpoled	Poled
(Fe/Nb)-O1	1.987(2)	1.970(1)
	2.029(2)	2.046(1)
(Fe/Nb)-O2	2.005(3)	1.890(1)
	2.016(3)	2.126(1)

343.3, 402.8, 431.7, 486.6, 574.2, 695.5, 780.0, and 858.2 cm^{-1} , respectively, which can be ascribed to the A_{1g} , E_g , F_{1g} , $4F_{1u}$, $2F_{2g}$, and F_{2u} optical phonon modes for a simplified cubic perovskite ABO_3 lattice in three dimensions with two types of cations at B -position.¹⁷ The tentative assignments of the observed modes, as shown in Fig. 6, were made based on the previous reports for unpoled PFN or for similar Pb based perovskites.¹⁷⁻²⁰ The modes, located in the region $700-850\text{ cm}^{-1}$ correspond to symmetric and asymmetric stretching vibrations of oxygen octahedra around Fe/Nb atoms of Nb-O-Nb (A_{1g} - 780.0 cm^{-1}), Nb-O (E_g - 858.2 cm^{-1}), and Nb-O-Nb (F_{1u} - 695.5 cm^{-1}) symmetry corresponds to monoclinic phase. The region of $400-530\text{ cm}^{-1}$ corresponds to the bending O-Fe/Nb-O vibrations of F_{2g} (574.2 cm^{-1}) and F_{1u} (486.6 and 431.7 cm^{-1}) symmetry. The modes at the region of $200-400\text{ cm}^{-1}$ are related to Pb-O bond stretching vibrations of F_{2u} symmetry (402.8 cm^{-1}), Fe/Nb-cation localized mode of F_{1u} symmetry (281.1 cm^{-1}), and the rotational mode of Fe/Nb-O₆ octahedra of F_{1g} symmetry (242.7 cm^{-1}). As can be observed in Fig. 6, it is worth mentioning that Raman spectra of unpoled PFN are almost similar to the spectra of relaxors from the same family,²¹⁻²³ where the peak at 780.0 cm^{-1} is well separated from other modes. The mode at $\sim 780.0\text{ cm}^{-1}$ is generally assigned as the Nb-O-Fe stretching mode, in analogy with the Nb-O-Mg stretching mode in $\text{Pb}(\text{Mg}_{1/3}\text{Nb}_{2/3})\text{O}_3$,^{24,25} being a characteristic peak in the Pb-based complex perovskite series. For instance, Pb is never found at its ideal Wyckoff position.^{8,26} Also, the cations of

TABLE I. Structural parameters such as cell constants, profile-fitting parameters for PFN sample before and after poling, obtained from the Rietveld analysis of the ND patterns.

PFN at 300 K	a (\AA)	b (\AA)	c (\AA)	β (deg)	Volume (\AA^3)	R_{Bragg}	R_f	R_{wp}	χ^2
Unpoled	5.6748(3)	5.6730(3)	4.0154(3)	89.97(2)	129.27(1)	9.4	5.2	6.7	5.0
Poled	5.6747(3)	5.6753(3)	4.0157(3)	89.96(2)	129.33(1)	11.4	6.4	4.4	3.3

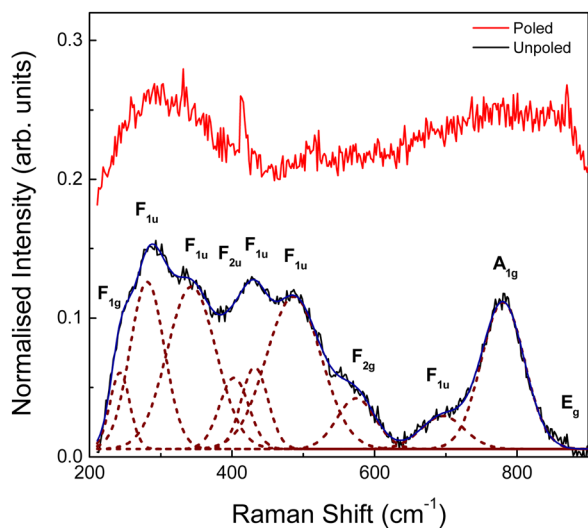


FIG. 6. Raman spectra for unpoled and poled samples of $\text{Pb}(\text{Fe}_{0.5}\text{Nb}_{0.5})\text{O}_3$ measured at room temperature.

Fe^{3+} and Nb^{5+} present local ordering within a disordered matrix.²⁷

As can be clearly seen in the said figure, the general aspects of the Raman spectra show a marked change for the poled PFN. These changes clearly indicate change at the octahedral site.^{17–20} In perspective of this, the ferroelectric ordering has enhanced. From the figure, it can be seen that in the poled sample Pb–O or O–Nb–O modes are more active than in the unpoled case. It was reported^{17–19} that the bands between 500 cm^{-1} and 900 cm^{-1} were of great importance for evaluating the B-site ordering in Pb-based multiferroics. Garcia-Flores *et al.*²⁰ reported that peak at 791 cm^{-1} indicates a possible indirect magnetic nature of these modes due to the presence of Fe^{3+} cations in the octahedral B site in PFN which exhibits both ferroelectric and magnetic properties. Indeed, such a magnetic ordering can cause spontaneous magnetostriction, that is, atomic displacements.

Poled PFN shows the remarkably enhanced modes located in the region $700\text{--}850\text{ cm}^{-1}$ corresponding to stretching vibrations of oxygen octahedra around Fe/Nb atoms of A_{1g} (780.0 cm^{-1}), E_g (858.2 cm^{-1}), and F_{1u} (695.5 cm^{-1}) symmetry corresponds to monoclinic phase. It can also be seen from Fig. 6 that the band around 780 cm^{-1} has become completely broad. This is matching well with the report of Garcia-Flores *et al.*²⁰ The electric poling showed a strong control on the Nb–O–Fe stretching mode, which indicates that after poling, the magnetic modes are deactivated and pronounced active modes are related to the ferroelectric ordering.

IV. CONCLUSIONS

In the present work, it has been shown that the magnetic and structural properties of $\text{Pb}(\text{Fe}_{0.5}\text{Nb}_{0.5})\text{O}_3$ can be controlled by poling the sample at room temperature (in the ferroelectric state). In PFN sample, Fe–O bonding controls the magnetism part, whereas the ferroelectric contribution comes largely due to Nb–O bonding. The combined

results of neutron diffraction, Raman spectroscopy, and magnetization measurements clearly show that Fe/Nb–O bonding is influenced by poling, resulting in the strengthening of the ferroelectric order however with reduction in the magnetism at room temperature. At low temperatures, there is reduction in the magnetic anisotropy in the electrically poled sample. Therefore, in the present system, electric field control of magnetism can be an ideal recipe for magnetic switching among other spintronic based applications.

ACKNOWLEDGMENTS

The authors would like to thank M. Venugopal (UGC-DAE CSR, Mumbai) for making the sample cell for *dc* electrical poling. S.M. and B.A. would like to thank DST PURSE program for providing the Raman Spectroscopy measurement facility at Department of Physics, Bangalore University, Bengaluru and UGC-DAE CSR (Mumbai centre) for providing financial support in the form of a collaborative research project (Nos. CRS-M-159 and CRS-M-200).

- ¹Z. Wang, Y. Yang, R. Viswan, J. Li, and D. Viehland, *Appl. Phys. Lett.* **99**, 043110 (2011).
- ²F. Zavaliche, H. Zheng, L. Mohaddes-Ardabili, S. Y. Yang, Q. Zhan, P. Shafer, E. Reilly, R. Chopdekar, Y. Jia, P. Wright, D. G. Schlom, Y. Suzuki, and R. Ramesh, *Nano Lett.* **5**, 1793 (2005).
- ³C. Zhang, F. Wang, C. Dong, C. Gao, C. Jia, C. Jiang, and D. Xue, *Nanoscale* **7**, 4187 (2015).
- ⁴T. Zhao, A. Scholl, F. Zavaliche, K. Lee, M. Barry, A. Doran, M. P. Cruz, Y. H. Chu, C. Ederer, N. A. Spaldin, R. R. Das, D. M. Kim, S. H. Baek, C. B. Eom, and R. Ramesh, *Nat. Mater.* **5**, 823 (2006).
- ⁵M. Fiebig, *J. Phys. D* **38**, R123 (2005).
- ⁶N. A. Spaldin and M. Fiebig, *Science* **309**, 391 (2005).
- ⁷B. Narayana Rao, A. N. Fitch, and R. Ranjan, *Phys. Rev. B* **87**, 060102R (2013).
- ⁸S. A. Ivanov, R. Tellgren, H. Rundlof, N. W. Thomas, and S. Ananta, *J. Phys.: Condens. Matter* **12**, 2393 (2000).
- ⁹A. Falqui, N. Lampis, A. Geddo-Lehmann, and G. Pinna, *J. Phys. Chem.* **109**, 22967 (2005).
- ¹⁰R. K. Mishra, R. N. P. Choudhary, and A. Banerjee, *J. Phys.: Condens. Matter* **22**, 025901 (2010).
- ¹¹M. H. Lente, J. D. S. Guerra, G. K. S. de Souza, B. M. Fraygola, C. F. V. Raigoza, D. Garcia, and J. A. Eiras, *Phys. Rev. B* **78**, 054109 (2008).
- ¹²V. V. Bhat, A. M. Umarji, V. B. Shenoy, and U. V. Waghmare, *Phys. Rev. B* **72**, 014104 (2005).
- ¹³S. Matteppanavar, S. Rayaprol, K. Singh, V. R. Reddy, and B. Angadi, *J. Mater. Sci.* **50**, 4980 (2015) and references there in.
- ¹⁴V. Siruguri, P. D. Babu, M. Gupta, A. V. Pimpale, and P. S. Goyal, *Pramana J. Phys.* **71**, 1197 (2008).
- ¹⁵H. Guo, C. Ma, X. Liu, and X. Tan, *Appl. Phys. Lett.* **102**, 092902 (2013).
- ¹⁶M. A. Carpenter, J. A. Schiemer, I. Lascu, R. J. Harrison, A. Kumar, R. S. Katiyar, N. Ortega, D. A. Sanchez, C. Salazar Mejia, W. Schnelle, M. Echizen, H. Shinohara, A. J. F. Heap, R. Nagarathnam, S. E. Dutton, and J. F. Scott, *J. Phys.: Condens. Matter* **27**, 285901 (2015).
- ¹⁷D. P. Kozlenko, S. E. Kichanov, E. V. Lukin, N. T. Dang, L. S. Dubrovinsky, H.-P. Liermann, W. Morgenroth, A. A. Kamynin, S. A. Gridnev, and B. N. Savenko, *Phys. Rev. B* **89**, 174107 (2014).
- ¹⁸B. Mihailova, R. J. Ange, A.-M. Welsch, J. Zhao, J. Enge, C. Paulmann, M. Gospodinov, H. Ahsbahs, R. Stosch, B. Güttler, and U. Bismayer, *Phys. Rev. Lett.* **101**, 017602 (2008).
- ¹⁹B. Mihailova, B. Maier, C. Paulmann, T. Malcherek, J. Ihringer, M. Gospodinov, and R. Stosch, *Phys. Rev. B* **77**, 174106 (2008).
- ²⁰A. F. Garcia-Flores, D. A. Tenne, Y. J. Choi, W. J. Ren, X. X. Xi, and S. W. Cheong, *J. Phys.: Condens. Matter* **23**, 015401 (2011).
- ²¹O. Svitelskiy, J. Toulouse, G. Yong, and Z. G. Ye, *Phys. Rev. B* **68**, 104107 (2003).

- ²²M. Zhu, C. Chen, J. Tang, Y. Hou, H. Wang, H. Yan, W. Zhang, J. Chen, and W. Zhang, *J. Appl. Phys.* **103**, 084124 (2008).
- ²³A. Lebon, M. El Marssi, R. Farhi, H. Dammak, and G. Calvarin, *J. Appl. Phys.* **89**, 3947 (2001).
- ²⁴E. Husson, L. Abello, and A. Morell, *Mater. Res. Bull.* **25**, 539 (1990).
- ²⁵S. A. Prosandeev, E. Cockayne, B. P. Burton, S. Kamba, J. Petzelt, Y. Yuzyuk, R. S. Katiyar, and B. S. Vakhrushev, *Phys. Rev. B* **70**, 134110 (2004).
- ²⁶N. Lampis, P. Sciau, and A. G. Lehmann, *J. Phys.: Condens. Matter* **11**, 3489 (1999).
- ²⁷Y. Yang, J.-M. Liu, H. B. Huang, W. Q. Zou, P. Bao, and Z. G. Liu, *Phys. Rev. B* **70**, 132101 (2004).